Canonical and microcanonical Monte Carlo simulations of lattice-gas mixtures

Carlos E. Fiore,[a] Vera B. Henriques, and Mario J. de Oliveira
Instituto de Física, Universidade de São Paulo, Caixa Postal 66318, 05315-970 São Paulo, Brazil

(Received 30 May 2006; accepted 11 September 2006; published online 27 October 2006)

We propose strict canonical and microcanonical Monte Carlo algorithms for an arbitrary lattice-gas binary mixture. We deduce formulas that allow us to obtain field quantities over the ensembles in which their conjugate extensive quantities are conserved. As an example, we have considered a lattice-gas mixture that is equivalent to the spin-1 Blume-Emery-Griffiths model [Phys. Rev. A **4**, 1071 (1971)]. For a finite system and near a phase coexistence, the field as a function of its extensive conjugate shows a loop that disappears in the thermodynamic limit giving rise to the usual tie line. The first-order phase transition was determined by the use of three criteria. © *2006 American Institute of Physics*. [DOI: 10.1063/1.2359435]

I. INTRODUCTION

According to Gibbs' statistical mechanics, it is possible, in principle, to use distinct ensembles to evaluate the thermodynamic properties of a given system, since the properties will be the same, in the thermodynamic limit.[1] The distinguishing feature of a given ensemble is that if a quantity is held fixed, its conjugate quantity will be a fluctuating variable. A quantity held fixed may be either an extensive or a field quantity. In the study of lattice spin models the use of Monte Carlo algorithms is common, in which all fixed quantities are fields, except one which must be extensive. In this paper we propose Monte Carlo algorithms in which two or more extensive variables are held fixed.

Since there are few problems in the statistical mechanics of interacting systems for which we can find an exact solution, Monte Carlo simulations are important tools for the analysis of models in statistical mechanics. Moreover, Monte Carlo simulations can be performed in any ensemble if one is able to set up the appropriate algorithm. For example, the one-component lattice-gas model, or Ising model, has been simulated in the grand-canonical ensemble,[2–5] in the canonical ensemble,[6,7] and in the microcanonical ensemble.[8] When a field quantity is held fixed, the calculation of its conjugate extensive quantity poses no problem. On the other hand, if an extensive quantity is held fixed, then the calculation of its conjugate field quantity may not be easily obtained. This problem is overcome here by the use of a procedure already introduced[8] which allows us to deduce the appropriate formulas for calculating a field quantity.

In spite of the equivalence of the ensembles, there are cases in which the use of a given ensemble may be more appropriate. A situation that illustrates this occurs when one desires to compare theoretical and experimental results, since experiments are performed in a specific ensemble. For example, experiments involving solutions of molecules, such as surfactant solutions, for which phase separation may be present,[7] it may be more advantageous to use the canonical ensemble, because in general these experiments are performed by maintaining the temperature and the concentration of molecules constant. Also, in case of polymer dilute solutions, it may not be trivial to implement grand-canonical simulations.[9]

Concerning the performance of numerical simulations, grand-canonical ensembles are usually generated by one-flip algorithms such as the dynamics of Metropolis *et al.*[2] and Glauber.[3] Although these algorithms are general and relatively easy to implement, they present hysteretic effects when used to determine first-order transitions, preventing a precise location of transition point. In the last years, several techniques have been proposed[10,11] to circumvent this fact, such as the use of cluster algorithms.[4,5,12] Several studies have shown the efficiency of using this technique to not only eliminate metastability in first-order transitions but also to reduce the critical slowing down in continuous phase transitions. However, these algorithms are specialized. Each model considered requires a specific cluster algorithm that takes account of the appropriate transitions. In some cases, such as antiferromagnetic models in a triangular lattice, *a priori* it is not possible to develop an efficient cluster algorithm. On the other hand, our approach is general and valid for any lattice-gas mixture model and, in particular, for the model considered here which is equivalent to the spin-1 Blume-Emery-Griffiths model.[13]

In the simulation of systems that display phase transitions, finite size effects are important. These effects have been investigated thoroughly for critical and first-order transitions in ensembles where the field variables are fixed. The situation in which the extensive variable is fixed is much less studied. In this case the field quantity as a function of its conjugate quantity exhibits a loop that is shown to disappear in the thermodynamic limit giving rise to the usual tie line. An appropriate treatment of loops has not been described in the literature. Therefore the comparison of results in different ensembles may lead to new methods for establishing phase transition lines or phase coexistence regions.

[a]Electronic mail: fiore@if.usp.br

Our aim here consists also of using a procedure[8] that allows us to obtain the field quantities with respect to both canonical and microcanonical ensembles for an arbitrary lattice-gas mixture of two components. The model has several applications, as in the study of solid-liquid-gas systems, liquid crystal mixtures, semiconductor alloys, and others.[13] It displays phase diagrams with very different structures.[14] In general, it is used to describe the behavior of systems whose phase transitions are governed by two mechanisms: symmetry breaking and density fluctuations.[13,14] We have described three criteria that can be used to identify and analyze first-order transitions in the ensembles whose extensive variables are strictly constant.

The algorithms we propose here are defined as follows. At each time step, two sites of the lattice having distinct values of the occupation variable are chosen at random. The two chosen sites need not be nearest neighbors. Actually they may be any pair of sites of the lattice. The canonical distribution is generated by interchanging their occupation variables with probability $\min\{1,\exp(-\beta\Delta\mathcal{H})\}$ where $\Delta\mathcal{H}$ is the change of energy due to the interchanging and $\beta=1/k_BT$ with T being the temperature and k_B the Boltzmann constant. The microcanonical distribution is generated by performing the interchanging only when the change of energy is null.

II. SPIN REPRESENTATION OF THE LATTICE-GAS MIXTURE

It is well known that a lattice-gas model composed of two species A and B with vacancies can be represented in terms of a spin-1 model.[13] Let us consider a mixture of species A and B sitting on a regular square lattice with $V=L\times L$ sites. To each site i of the lattice we attach a variable σ_i which takes, the values of 1, 0, and −1 according to whether the site i has a particle of species A, is vacant, or a particle of species B, respectively. A configuration of the system is denoted by $\sigma=(\sigma_1,\sigma_2,\ldots,\sigma_i,\ldots,\sigma_V)$, and the Hamiltonian $\mathcal{H}(\sigma)$, which is a sum of pair interaction energy, is given by

$$\mathcal{H}=-J\sum_{(i,j)}\sigma_i\sigma_j-K_1\sum_{(i,j)}\sigma_i^2\sigma_j^2-K_2\sum_{(i,j)}(\sigma_i\sigma_j^2+\sigma_i^2\sigma_j), \quad (1)$$

where the summation is over the nearest neighbor pair of sites. The parameters J, K_1, and K_2 are related to the interaction energies between particles placed at neighboring sites of the lattice as follows:

$$J=(\epsilon_{AA}+\epsilon_{BB}-2\epsilon_{AB})/4, \quad (2)$$

$$K_1=(\epsilon_{AA}+\epsilon_{BB}+2\epsilon_{AB})/4, \quad (3)$$

and

$$K_2=(\epsilon_{AA}-\epsilon_{BB})/2, \quad (4)$$

where $-\epsilon_{AA}$, $-\epsilon_{BB}$, and $-\epsilon_{AB}$ are the energies of interaction between species AA, BB, and AB, respectively.

It is convenient to define the following quantities:

$$\mathcal{M}=\sum_{i=1}^{V}\sigma_i \quad (5)$$

and

$$\mathcal{Q}=\sum_{i=1}^{V}\sigma_i^2. \quad (6)$$

These two quantities are related to the number of particles N_A of species A and the number of particles N_B of species B. The quantity $\mathcal{Q}$ is just the total number of particles,

$$\mathcal{Q}=N_A+N_B, \quad (7)$$

and $\mathcal{M}$ is the difference between the number of particles of species A and B,

$$\mathcal{M}=N_A+N_B. \quad (8)$$

The microcanonical ensemble is defined in such a way that the probability $P_{\text{inc}}(\sigma)$ of a configuration σ is the same for all configurations such that $\mathcal{H}(\sigma)$, $\mathcal{M}(\sigma)$, and $\mathcal{Q}(\sigma)$ are held constant. The probability distribution for this ensemble is given by

$$P_{\text{inc}}(\sigma)=\frac{1}{W}\delta(\mathcal{H}(\sigma),U)\delta(\mathcal{M}(\sigma),M)\delta(\mathcal{Q}(\sigma),Q), \quad (9)$$

where U is the fixed value of the energy, M is the fixed value of the difference N_A-N_B and Q is the fixed value of the total number of particles N_A+N_B, and $\delta(x,y)$ denotes the Kronecker delta.

In the canonical ensemble, $\mathcal{M}(\sigma)$ and $\mathcal{Q}(\sigma)$ are held constant but not $\mathcal{H}(\sigma)$. In this case the probability $P_c(\sigma)$ of a configuration σ such that $\mathcal{M}(\sigma)$ and $\mathcal{Q}(\sigma)$ are constant is given by

$$P_c(\sigma)=\frac{1}{Z}\exp\{-\beta\mathcal{H}(\sigma)\}\delta(\mathcal{M}(\sigma),M)\delta(\mathcal{Q}(\sigma),Q), \quad (10)$$

where $\beta=1/k_BT$.

In the grand-canonical ensemble the quantities $\mathcal{M}(\sigma)$ and $\mathcal{Q}(\sigma)$ are also allowed to fluctuate and the probability distribution $P(\sigma)$ of the configuration σ is given by

$$P(\sigma)=\frac{1}{\Xi}\exp\{-\beta[\mathcal{H}(\sigma)-H\mathcal{M}(\sigma)+D\mathcal{Q}(\sigma)]\}. \quad (11)$$

where H is the field conjugated to $M=\langle\mathcal{M}(\sigma)\rangle$ and D is the field conjugated to $Q=\langle\mathcal{Q}(\sigma)\rangle$. They are related to the chemical potentials μ_A and μ_B of the species A and B, respectively, by

$$H=\frac{\mu_A-\mu_B}{2} \quad (12)$$

and

$$D=-\frac{\mu_A+\mu_B}{2}. \quad (13)$$

III. GRAND-CANONICAL ENSEMBLE

If the Monte Carlo simulation is performed in the grand-canonical ensemble then the quantities $U=\langle\mathcal{H}\rangle$, $M=\langle\mathcal{M}\rangle$, and $Q=\langle\mathcal{Q}\rangle$ can be calculated simply as the averages of the well defined state functions $\mathcal{H}(\sigma)$, $\mathcal{M}(\sigma)$, and $\mathcal{Q}(\sigma)$. If, however, an ensemble is used in which $\mathcal{H}$, $\mathcal{M}$, and $\mathcal{Q}$ are held fixed, we have to know how to determine their conjugate

variables, the temperature T and the fields H and D. In the following we will deduce the appropriate formulas that allows us to perform these calculations.

One may obtain relations between the field variables H and D and average quantities $M=\langle \mathcal{M}(\sigma)\rangle$ and $Q=\langle \mathcal{Q}(\sigma)\rangle$ by considering relations between probabilities $P(\sigma)$ of different microscopic states σ. We start by writing the ratio between the probability of configuration $\sigma^{i,0}$, in which $\sigma_i=0$, and configuration $\sigma^{i,+}$, in which $\sigma_i=+1$. It is given by

$$\frac{P(\sigma^{i,+})}{P(\sigma^{i,0})}=\exp\{\beta[\phi_i^+(\sigma)+H-D]\}, \tag{14}$$

with

$$\phi_i^+=(J+K_2)\sum_\delta \sigma_{i+\delta}+(K_1+K_2)\sum_\delta \sigma_{i+\delta}^2, \tag{15}$$

where the summation is over the nearest neighbor sites of site i. This ratio can written as

$$P(\sigma^{i,+})=e^{\beta(H-D)}P(\sigma^{i,0})\exp\{\beta\phi_i^+(\sigma)\} \tag{16}$$

or yet as

$$\langle\delta(\sigma_i,1)\rangle=e^{\beta(H-D)}\langle\delta(\sigma_i,0)\exp\{\beta\phi_i^+(\sigma)\}\rangle, \tag{17}$$

if we sum over all possible configurations σ, where $\langle\ldots\rangle$ denotes an average over the grand-canonical ensemble. From this equation the relation follows:

$$e^{-\beta(H-D)}=\frac{\langle\delta(\sigma_i,0)\exp\{\beta\phi_i^+(\sigma)\}\rangle}{\langle\delta(\sigma_i,1)\rangle}. \tag{18}$$

By an analogous reasoning, if we started from the ratio

$$\frac{P(\sigma^{i,-})}{P(\sigma^{i,0})}=\exp\{\beta[\phi_i^-(\sigma)-H-D]\}, \tag{19}$$

where

$$\phi_i^-=-(J-K_2)\sum_\delta \sigma_{i+\delta}+(K_1-K_2)\sum_\delta \sigma_{i+\delta}^2, \tag{20}$$

we would reach the relation

$$e^{\beta(H+D)}=\frac{\langle\delta(\sigma_i,0)\exp\{\beta\phi_i^-(\sigma)\}\rangle}{\langle\delta(\sigma_i,-1)\rangle}. \tag{21}$$

Dividing Eqs. (14) and (19) we obtain the ratio

$$\frac{P(\sigma^{i,+})}{P(\sigma^{i,-})}=\exp\{2\beta[\phi_i(\sigma)+H]\}, \tag{22}$$

where

$$\phi_i(\sigma)=J\sum_\delta \sigma_{i+\delta}+K_2\sum_\delta \sigma_{i+\delta}^2, \tag{23}$$

from which we reach the relation

$$e^{-2\beta H}=\frac{\langle\delta(\sigma_i,-1)\exp\{2\beta\phi_i(\sigma)\}\rangle}{\langle\delta(\sigma_i,1)\rangle}. \tag{24}$$

The above relation is identical to that obtained for the ordinary lattice-gas model or the Ising model in the spin language.[8]

Now let us denote by E any one of the possible values that $\phi_i^+(\sigma)$ may assume and let us multiply both sites of Eq. (16) by $\delta(\phi_i^+(\sigma),E)$ to get

$$P(\sigma^{i,+})\delta(\phi_i^+(\sigma),E)=e^{\beta(E+H-D)}P(\sigma^{i,0})\delta(\phi_i^+(\sigma),E). \tag{25}$$

After summing over all possible configurations σ the following relation can be reached:

$$e^{-\beta(E+H-D)}=\frac{\langle\delta(\sigma_i,0)\delta(\phi_i^+(\sigma),E)\rangle}{\langle\delta(\sigma_i,1)\delta(\phi_i^+(\sigma),E)\rangle}. \tag{26}$$

From Eq. (22), we get the expression

$$P(\sigma^{i,+})=P(\sigma^{i,-})\exp\{2\beta[\phi_i(\sigma)+H]\}. \tag{27}$$

If we multiply both sides of this equation by $\delta(\phi_i(\sigma),E)$, where E denotes now the possible values assumed by $\phi_i(\sigma)$, and summing over all configurations, we reach the following relation:

$$e^{-2\beta(E+H)}=\frac{\langle\delta(\sigma_i,-1)\delta(\phi_i(\sigma),E)\rangle}{\langle\delta(\sigma_i,1)\delta(\phi_i(\sigma),E)\rangle}. \tag{28}$$

Thus, we have written down relations between field variables, such as the temperature T and the fields H and D, and certain averages calculated in the grand-canonical ensemble.

IV. MICROCANONICAL AND CANONICAL ENSEMBLES

In the following, we resort to the equivalence of ensembles in order to write relations between field variable and averages calculated in the canonical or microcanonical ensemble. This extends to spin-1 models the procedure used for the Ising model.[8] In the canonical ensemble, the temperature T and the particle numbers N_A and N_B are constant which means that $\mathcal{M}$ and $\mathcal{Q}$ are held fixed. The canonical probability distribution $P_c^-(\sigma)$ is given by Eq. (10).

Assuming the equivalence of ensembles, Eqs. (18) and (21) may be rewritten as

$$\exp\{-\beta(H-D)\}=\frac{\langle\delta(\sigma_i,0)\exp\{\beta\phi_i^+(\sigma)\}\rangle_c}{\frac{1}{2}(q+m)} \tag{29}$$

and

$$\exp\{\beta(H+D)\}=\frac{\langle\delta(\sigma_i,0)\exp\{\beta\phi_i^-(\sigma)\}\rangle_c}{\frac{1}{2}(q-m)}, \tag{30}$$

where $\langle\ldots\rangle_c$ denotes an average in the canonical ensemble, $q=Q/V$, and $m=M/V$. These formulas allow us to obtain H and D from the canonical distribution and from them the chemical potentials μ_A and μ_B by means of Eqs. (12) and (13).

In the microcanonical ensemble, the total energy of the system $\mathcal{H}(\sigma)$ and the quantities $\mathcal{M}(\sigma)$ and $\mathcal{Q}(\sigma)$ are held fixed. The probability distribution $P_{\mathrm{mc}}(\sigma)$ is given by Eq. (9). Appealing to the equivalence of ensembles, we use Eq. (26) to write

$$\exp\{-\beta(E+H-D)\} = \frac{\langle \delta(\sigma_i,0)\delta(\phi_i^+(\sigma),E)\rangle_{\rm mc}}{\langle \delta(\sigma_i,1)\delta(\phi_i^+(\sigma),E)\rangle_{\rm mc}}. \quad (31)$$

Analogously, we can write a second relation for the microcanonical ensemble by using Eq. (28),

$$\exp\{-2\beta(E+H)\} = \frac{\langle \delta(\sigma_i,-1)\delta(\phi_i(\sigma),E)\rangle_{\rm mc}}{\langle \delta(\sigma_i,1)\delta(\phi_i(\sigma),E)\rangle_{\rm mc}}, \quad (32)$$

where $\langle \ldots \rangle_{\rm mc}$ denotes an average over the microcanonical ensemble. These formulas allow us to obtain the temperature T and the fields H and D for the microcanonical ensemble.

It is worth mentioning that formulas relating a field quantity to an average over an ensemble in which the conjugate extensive quantity is held fixed have been considered for continuous systems.[15,16] For lattice systems analogous relations have also been obtained.[8,16]

Other approaches to describe microcanonical ensembles have been proposed in the literature. Creutz[17] has generated a microcanonical ensemble by assuming a canonical distribution of the energies carried by a "demon," whereas Lang and Stauffer[18] used an empirical energy-temperature relationship determined by a canonical Monte Carlo simulation. We remark that these approaches are distinct from ours.

V. NUMERICAL SIMULATIONS

We have performed numerical simulations of the lattice gas mixture with the total energy $\mathcal{H}(\sigma)$ given by Eq. (1). We will take the values $K_2=0$ and $K_1=3J$ for energy constants, which correspond to symmetric interaction energies $\epsilon_{AA}=\epsilon_{BB}=2\epsilon_{AB}$. The corresponding phase diagram in the plane T vs D is well known, and it has been determined by Hoston and Berker[14] by means of mean field analysis.

For $H=0$, the concentration of species A and B is equal, whereas $H>0$ ($H<0$) favor the concentration of species A (B). Concerning the analysis at $H=0$, small T and D, there is the phase separation of species A and B, respectively. Increasing D at low temperatures, the coexistence of three phases (rich at species A and B and vacancies) takes place, whereas for higher values of D only the phase rich at vacancies occurs. The phases rich at species A and B and rich at vacancies may be interpreted as two liquid phases and a gas phase, respectively, in analogy with the phase diagram of a simple fluid.

In the low temperature regime, when one increases D, the phase transition between the liquid phases and the gas phase is first order and it occurs at $D=2z$ where z is the coordination number. In the present case of a square lattice, $z=4$. For higher temperatures, the model displays a triple point, a critical point, and a tricritical point from which comes out a line of critical points. We will concern our analysis at first-order phase transitions.

It is possible to study the phase diagram of the system by considering different variables. If we take the phase diagram in the space of intensive variables, the coexistence of phases and second order transitions will be represented by a single point at the diagram. If the phase diagram is plotted by considering an intensive variable and an extensive one, the coexistence of phases will now be described by a tie line, whereas a second-order transition corresponds to a point. However, as it will be shown subsequently, the tie line occurs only in the thermodynamic limit; for finite systems it is replaced by a loop.[19] In the next subsection, we will describe and analyze three distinct criteria that can be used to determine the phase diagrams.

A. Canonical ensemble

We simulated the lattice-gas mixture in a square lattice with periodic boundary conditions. The simulations were performed for fixed values of $\mathcal{M}$ and $\mathcal{Q}$. In all simulations we have considered $\mathcal{M}=0$. Thus, the total number of species A is equal to the total number of species B.

The actual Monte Carlo simulation begins by distributing $N_A=(\mathcal{Q}+\mathcal{M})/2$ and $N_B=(\mathcal{Q}-\mathcal{M})/2$ particles over the lattice. Since the total number of particles is strictly constant, the total number of vacant sites $V-(N_A+N_B)$ is also constant. For a given initial configuration (in our case, we started from a disordered initial configuration), one of the three possible transitions is chosen with equal probability. Next, two sites of the lattice describing the chosen transition are selected at random. The chosen sites interchange their occupation variables obeying the transition rate,

$$w = \min\{1, \exp(-\beta\Delta\mathcal{H})\}, \quad (33)$$

where $\Delta\mathcal{H}$ is the increase of the energy of the system after the interchange step. It is important to observe that this rate transition satisfies the detailed balance condition. We used system sizes ranging from $L=30$ to $L=80$ and 10^7 Monte Carlo steps to evaluate the appropriate averages. Here a Monte Carlo step corresponds to V possible interchanges between the chosen occupation variables. The first criterion used here consists of obtaining the transition point by means of analysis of the specific heat. The specific heat $C_{q,m}$ at fixed m and q is related to the total energy $\mathcal{H}$ by means of the relation

$$C_{q,m} = \frac{1}{Vk_BT^2}[\langle \mathcal{H}^2\rangle_c - \langle \mathcal{H}\rangle_c^2]. \quad (34)$$

In Fig. 1, we plotted the specific heat $C_{q,m}$ versus the temperature T for $q=0.2$.

Under the condition of temperature T, q, and m held constant, starting from the coexistence of three phases we will arrive at a homogeneous phase for lower values of q or to the coexistence of two liquid phases, for higher values of q. For a system of size L, the crossing from one regime to another one is described by a maximum in the specific heat at T_L. We expect that, in the thermodynamic limit, the crossing between the two regimes is signed by a peak in the specific heat at T_0^*. However, in the thermodynamic limit, the specific heat $C_{q,m}$ does not become a delta-function singularity. This is expected in first-order transitions between two phases when the chemical potentials (fields) are held constant. Finite size analysis in this case is well established,[21] with the difference between the temperature T_L at which the specific heat is maximum and the temperature of the phase transition in the thermodynamic limit T_0^* decaying as L^{-2}.[12,20,21] The scale with the volume of the system is related

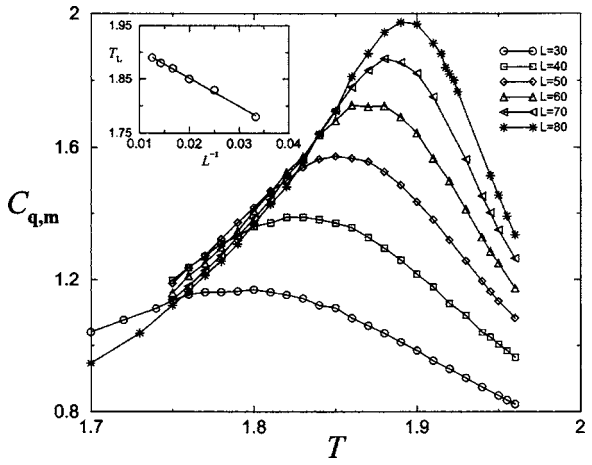

FIG. 1. Specific heat $C_{q,m}$ vs the temperature T for several system sizes L in the canonical ensemble. In the inset, we have plotted the temperature T_L when the specific heat is maximum, as function of L^{-1}.

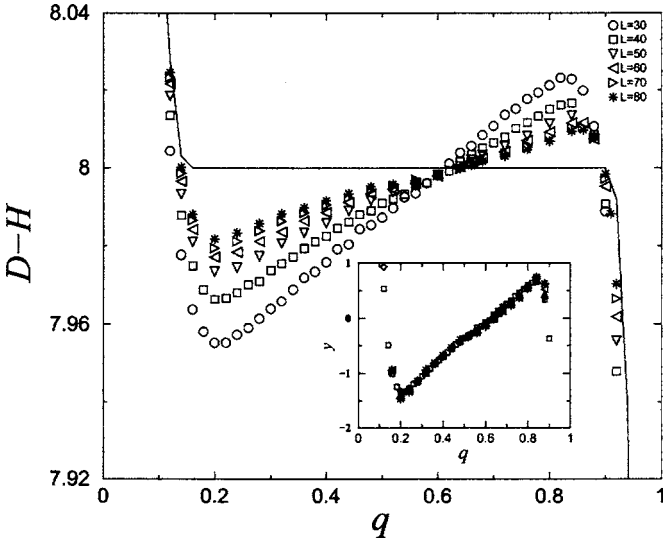

FIG. 2. Isotherms of field $D-H$ as function of the parameter q for several system sizes for $T=1.955$. The solid line is the extrapolation using Eq. (35). The inset shows the collapse of the same curves by using the equation $y=(\bar{D}_L-D_0^*)L$ vs q.

to the double Gaussian distribution of the energy near the transition, separated by a minimum of the probability distribution.

In the present case, the difference $T_L-T_0^*$ decays as L^{-1} when one increases L, as can be shown in the inset of Fig. 1. A reasoning for justifying a different scale behavior is that, in the present case, the energy is described by a single Gaussian distribution throughout. Using this asymptotic scale relation, we obtained the extrapolated temperature $T_0^*=1.956(3)$. We have also performed finite size analysis for the chemical potentials at the crossing between the two regimes in order to compare with available results, obtained from grand-canonical Monte Carlo simulations by means of a cluster algorithm.[20] For the temperature extrapolated above, the chemical potentials indeed exhibit the same dependence on the inverse of the system size L, whose extrapolated chemical potentials are $D_0^*=7.998(2)$ and $H_0^*=0.001(1)$. These estimates agree very well with $D_0^*=8.0001(1)$ and $H_0^*=0$, obtained from grand-canonical simulations by means of a cluster algorithm.[20] This method for determining the coexistence line has been repeated for other values of q. For $q=0.3$, the peak in the specific heat occurs at the extrapolated temperature $T_0^*=1.980(1)$ whose value of D_0^* is 8.002(1), in agreement with the estimate $D_0^*=7.998(2)$, evaluated for $q=0.2$.

The second procedure for determining the phase diagram consists of plotting isotherms of the chemical potential of the species, saying $D-H$, versus q, as shown in the Fig. 2. We can see, from Fig. 2, that isotherms exhibit loops at the coexistence of phase region, even for large L. To understand the origin of loops in the isotherms of chemical potential, let us consider the probability distribution in the grand-canonical ensemble. The loci of extrema of the grand-canonical distribution function produce the functions $D(Q,M)$ and $H(Q,M)$ for the canonical ensemble, whose maxima are associated with regions where $\partial D/\partial Q<0$ and minima where $\partial D/\partial Q>0$. The presence of more than one extreme in the probability distribution leads to loops for the field variables in the canonical ensemble. The reasoning proposed by Hill[23] to relate the loops of the chemical potential with the system size L is that the free energy of the system at the coexistence of phases has a term due to interface effects between the phases proportional to $V^{1/2}$, in two dimensions. This leads to the following expression for the minimum (or the maximum) of the chemical potential D_m^*:

$$D_m^*-D_0^*\sim L^{-1}, \tag{35}$$

where D_0^* is its asymptotic value. In the thermodynamic limit, the loops disappear. An analogous relation can be written down for the field H. Our data is clearly described by Eq. (35), which gives the asymptotic values $H_0^*=0.001(1)$ and $D_0^*=8.0008(3)$. These estimates are in excellent agreement with the values $H_0^*=0$ and $D_0^*=7.998(2)$ obtained from the specific heat analysis showed above.

Our data support that not only the maximum and the minimum D_m^*, but also all values of q inside the coexistence region, follow Eq. (35), as can be seen in Fig. 3. The inset of Fig. 2 shows the collapse of all curves in the coexistence region using the transformation $y=(\bar{D}_L-D_0^*)L$, where $\bar{D}_L\equiv D_L^*-H_L^*$ is the chemical potential obtained for a fixed q and fixed system size L. The collapse of all curves confirms the dependence of the fields on the inverse of the system size L, whose asymptotic values of D_0^* are compatible to 8.0008(3).

For higher values of q outside the coexistence region, the deviation of D from its asymptotic value also decays as $1/L$, as shown in Fig. 3. This can be understood by the fact that two liquid phases coexist and therefore the calculated quantities are also affected by interface phenomena.[23] For lower values of q outside the coexistence region, the deviation of D from its asymptotic value is not proportional to $1/L$ but to $1/L^2$, as shown in Fig. 3.

The third criterion consists of identifying the transition point by the crossing among the isotherms of chemical potential for different system sizes, as shown in Fig. 2. As we show in the Appendix, the crossing point is independent of lattice size and properly identifies coexistence. All curves

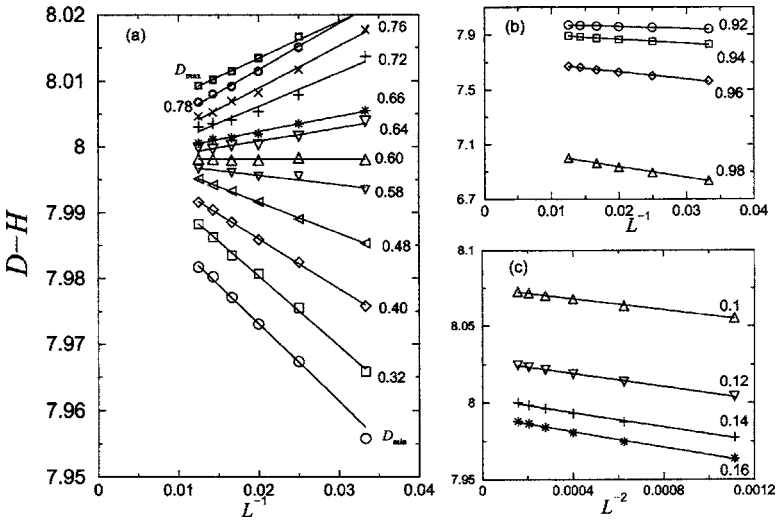

FIG. 3. Dependence of $D-H$ on L^{-1} in (a) and (b) and on L^{-2} in (c) for several values of q in the canonical ensemble for $T=1.955$.

cross at $D=8.000(2)$, in good agreement with the other two criteria described above. Let q_{gas} and q_{liq} be the densities of the phases poor and rich in species A and B, respectively. At this point the fraction

$$\alpha = \frac{q - q_{\mathrm{gas}}}{q_{\mathrm{liq}} - q_{\mathrm{gas}}} \tag{36}$$

equals 0.65(1). In the Appendix we demonstrate that the crossing among the isotherms occurs at $\alpha=2/3$, very close to the value $\alpha=0.65(1)$.

The crossing among the isotherms of q vs D is also observed in grand-canonical simulations with a cluster algorithm, and it occurs at the transition point $D=8.0$ and $\alpha=2/3$.[20] Although the crossing occurs at the same point for both ensembles, the behavior of the isotherms in distinct ensembles are very different. While in the canonical ensemble the isotherms possess loops, as shown in Fig. 2, in the grand-canonical ensemble the isotherms present no loops and are monotonic functions.[20] In the thermodynamic limit, the isotherms with loops coming from the canonical ensemble and the isotherms coming from the grand-canonical ensemble reduces to the same and unique isotherm with a tie line at the crossing point. We remark that if we use a Monte Carlo algorithm with local rules, such as a one-flip algorithm, to simulate the grand-canonical ensemble there will be no crossing due to the presence of hysteresis.[20] The second and third criteria described here has been verified for other values of temperatures. For $T=0.9$, the crossing among the isotherms occurs at about $\alpha=2/3$, whose value of D is also consistent to 8.0.

B. Microcanonical ensemble

To simulate the lattice-gas model with vacancies in the microcanonical ensemble we have also considered a square lattice and periodic boundary conditions. The system was simulated at total energy $\mathcal{H}$, with N_A and N_B strictly conserved. We started from an ordered initial state. In order to reach a state with the desired value of the energy which will be held fixed, we have performed at first only exchanges that increase the total energy. When the desired energy is reached, we start the actual simulation in which only exchanges that do not change the total energy will be performed.

After the system reached the steady state, we have calculated the temperature and the fields H and D using Eqs. (31) and (32). We considered here the same values of K_1 and K_2 of the previous section. Thus, from Eqs. (15) and (23), the possible values of E to be used in Eqs. (31) and (32) are $0, 2J, 4J, \ldots, 16J$ and $-4J, -3J, \ldots, 3J, 4J$, respectively.

To simplify the notation, the right-hand side of Eqs. (31) and (32) is renamed as $1/R_1$ and $1/R_2$, respectively. The quantity R_1 is the ratio between the average number of particles of type A with nearest neighbor energy nJ and the average number of empty sites with nearest neighbor energy nJ. The quantity R_2 is the ratio between the average number of particles A with nearest neighbor energy nJ and the average number of particles of type B with nearest neighbor energy nJ.

Extracting the logarithm of the Eqs. (31) and (32), we get the following relations, given in unities of J and k_B:

$$\ln R_1 = \frac{n}{T} + \frac{H - D}{T} \tag{37}$$

and

$$\ln R_2 = \frac{2n}{T} + \frac{2H}{T}. \tag{38}$$

In these forms, the temperature T and the fields H and D can be obtained from the two coefficients of these linear equations. In Figs. 4 and 5, we show a log plot of R_1 and R_2 for several values of n. The numerical data reveal that the quantities $\ln R_1$ and $\ln R_2$ are indeed linear in n, as expected. From the linear fitting we determine T, H, and D. The quantities were calculated using a lattice of size $L=90$ and $m=0$ and $q=2/3$.

In Figs. 4 and 5, all curves intercept at the points (8,0) and (0,0), respectively. This implies that, from Eqs. (37) and (38), $D=8$ and $H=0$ for all values of temperatures and system sizes. The independence on the system size for D and H for $m=0$ and $q=2/3$ agrees with the third criterion proposed

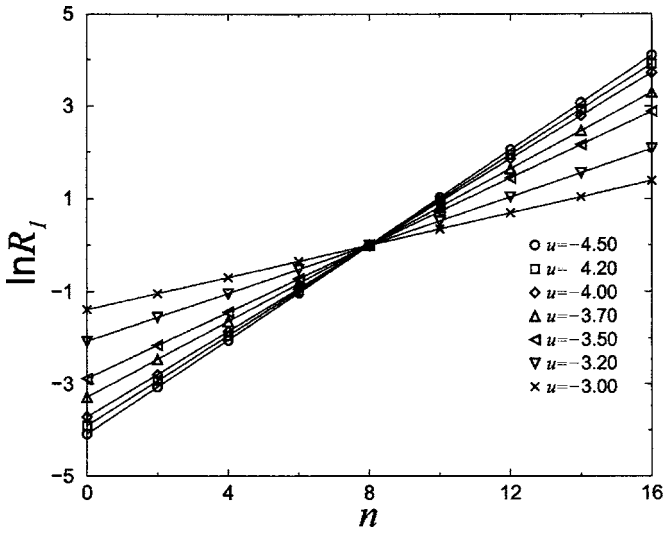

FIG. 4. Logarithm plot of R_1 vs n for several values of total energy per site u considering the square lattice with $L=90$, taking $m=0$ and $q=2/3$ for the lattice-gas model with vacancies.

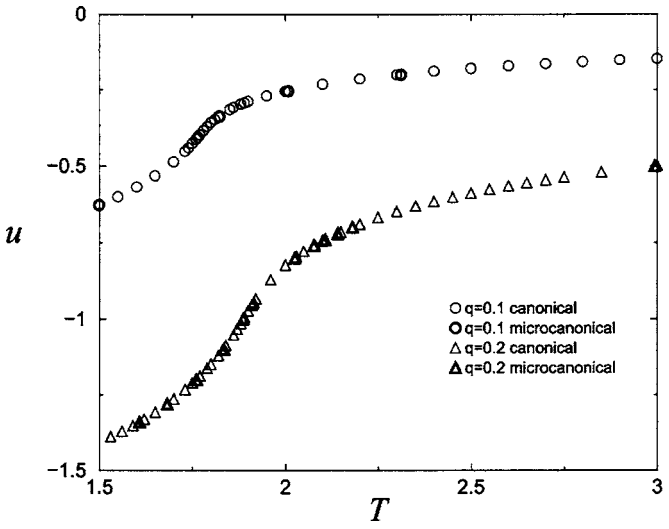

FIG. 6. Energy density u obtained from both canonical and microcanonical ensembles, for a square lattice of size $L=80$ and $m=0$, with $q=0.1$ (circles) and $q=0.2$ (triangles).

for analyzing isotherms in the canonical ensemble, showed previously. We remark that for $q \neq 2/3$, there is no crossing among the curves of the quantity $\ln R_1$.

To draw a comparison between the ensembles, we plotted in Fig. 6, the total energy per site u versus the temperature T for the canonical and microcanonical ensembles. We used a lattice size $L=80$ and the parameters $m=0$ and $q=0.2$. From our data, we see that the results coming from distinct ensembles agree very well, even for smaller system sizes. For example, in the canonical ensemble for fixed $T=1.800$, $m=0$, and $q=0.2$ we obtained the mean total energy $u=-1.1106(6)$. In the microcanonical ensemble for fixed total energy per site $u=-1.110\,56$ we obtained $T=1.801(1)$. Small discrepancies are due to finite size effects. Another comparison between the ensembles is done by plotting isotherms of D vs q for different temperatures, as shown in Fig. 7. In the low temperature regime, the isotherms in the plane D vs q, determined by the microcanonical Monte Carlo ensemble, also exhibit loops, as can be shown in Fig. 7.

Microcanonical simulations are also influenced by finite size effects. To verify the dependence of the field quantities on the system size L, we plotted the evaluated temperature T_L as a function of L^{-1} and L^{-2} for several values of u for $q=0.2$. As can be seen in Fig. 8, below T_0^* (obtained from the canonical ensemble), the deviation of T_L from its asymptotic value decays as L^{-1}, whereas above T_0^*, the deviation becomes proportional to L^{-2}, in agreement with the results by Shida *et al.*[8] for the microcanonical Ising model. Finite size analysis for the microcanonical ensemble proposed by Creutz[17] has been described by Desai *et al.*[22] for the Ising model.

VI. CONCLUSION

We introduced both canonical and microcanonical Monte Carlo algorithms that can be used for describing any

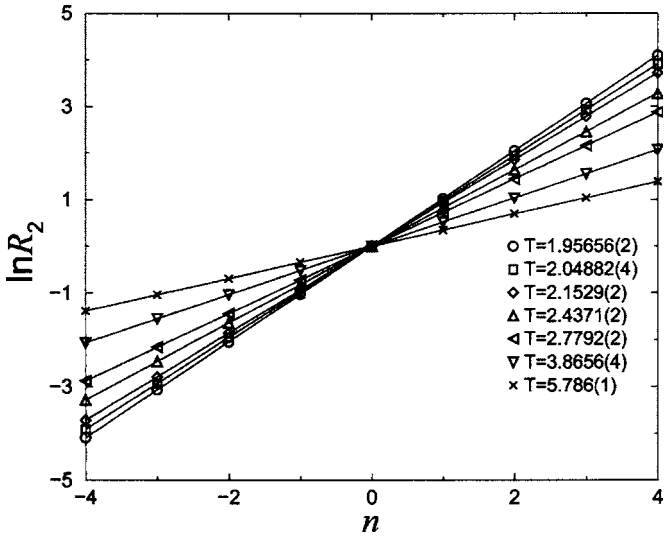

FIG. 5. Logarithm plot of R_2 vs n for several values of total energy per site u considering a square lattice with $L=90$, taking $m=0$ and $q=2/3$ for the lattice-gas model with vacancies.

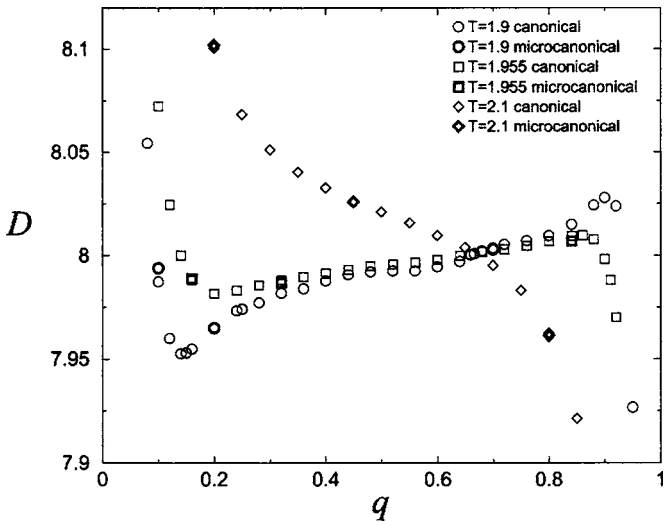

FIG. 7. Isotherms of D vs q obtained in the canonical and microcanonical ensembles at different temperatures. We considered here a lattice of size $L=80$.

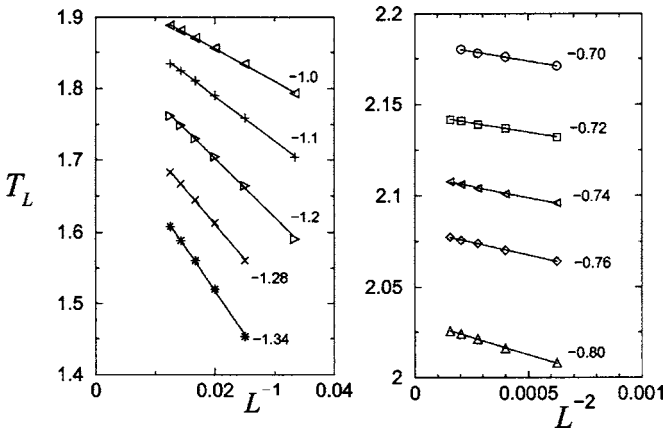

FIG. 8. Dependence of the temperature T_L on the system size L for several values of u and $q=0.2$ in the microcanonical ensemble. In the first and second graphs we plotted T_L vs L^{-1} and L^{-2}, respectively.

lattice-gas model with vacancies, equivalent to a spin-1 model. We deduced formulas that allow us to obtain the fields (chemical potentials) with respect to the canonical ensemble and the fields and temperature in the microcanonical ensemble. We described in detail three distinct criteria that can be used to identify first-order transitions in systems whose extensive variables are held fixed. For a finite system we have shown that near a coexistence the isotherms present loops that disappear in the thermodynamic limit, giving rise to the usual tie line characteristic of a first-order transition. For different system sizes, the isotherms cross at a point, which allows us to use it as a criterion to locate the first-order transition.

ACKNOWLEDGMENT

One of the authors (C.E.F.) acknowledges the financial support from Fundação de Amparo à Pesquisa do Estado de São Paulo (FAPESP) under Grant No. 03/01073-0.

APPENDIX: LOOPS IN THE ISOTHERMS OF THE CANONICAL ENSEMBLE AND THE COEXISTENCE CROSSING POINT

If the isotherms corresponding to a given temperature, near coexistence, is plotted in the plane of field versus density for different lattice sizes, they will cross at the same point. At this point they are thus independent of size and can be used as a reference for identifying coexistence. This can be proven by analyzing the probability distribution for densities near coexistence. Following arguments similar to Refs. 24 and 25, we may write the grand-canonical probability distribution of Q and M around the equilibrium values Q_0 and M_0 as

$$P(Q,M;D,H) \sim \exp\{-\beta\Psi_0(H,D)\} \times \exp\left\{-\frac{(Q-Q_0)^2}{2(X_D)_0}+\frac{(M-M_0)^2}{2(X_H)_0}\right\}, \tag{A1}$$

where $\Psi_0(H,D)$ is the grand-canonical potential and

$$X_D=-\frac{\partial Q}{\partial D}, \tag{A2}$$

$$X_H=\frac{\partial M}{\partial H}. \tag{A3}$$

Near the coexistence of n phases the distribution is constructed from n Gaussian functions. Next, we make use of density quantities $q=Q/V$, $m=M/V$, $\chi_D=X_D/V$, and $\chi_H=X_H/V$, to write the probability distribution *at* the three phase coexistence of gas ($q_0=q_{\rm gas}$, $m_0=0$) and rich A ($q_0=q_{\rm liq}$, $m_0=m_1$) or rich B ($q_0=q_{\rm liq}$, $m_0=-m_1$) as

$$P(q,m;D,H) \sim \exp\left\{-\beta V\left[\frac{(q-q_{\rm gas})^2}{2(\chi_D)_{\rm gas}}+\frac{m^2}{2(\chi_H)_{\rm gas}}\right]\right\} + 2\exp\left\{-\beta V\left[\frac{(q-q_{\rm liq})^2}{2(\chi_D)_{\rm liq}} + \frac{(m-m_1)^2}{2(\chi_H)_{\rm liq}}\right]\right\}. \tag{A4}$$

If we define $\bar{q}$ as the density at which the distribution has a minimum (by symmetry this minimum must be located at $m=0$), we obtain, to first order,

$$\frac{\bar{q}-q_{\rm gas}}{V^{-1}(\chi_D)_{\rm gas}}=-2\frac{\bar{q}-q_{\rm liq}}{V^{-1}(\chi_D)_{\rm liq}}, \tag{A5}$$

which makes the location of the minimum of the distribution independent of the lattice size L, since $V^{-1}\chi_D$ is of order unity. As a consequence, the field isotherms all cross at this point, which thus localizes the coexistence fields and corresponding tie lines. For the particular case we have studied, due to symmetry, $(\chi_D)_{\rm gas}=(\chi_D)_{\rm liq}$, from which follows

$$\bar{q}-q_{\rm gas}=\tfrac{2}{3}(q_{\rm liq}-q_{\rm gas}), \tag{A6}$$

or, comparing with Eq. (36), $\alpha=2/3$. In the case of the grand-canonical ensemble, hysteresis is obtained from Monte Carlo simulations that use local rules such as a one-spin flip algorithm. If, however, a cluster algorithm is adopted then the hysteresis is absent and a smooth variation of the isotherms is obtained.[20] In this case, isotherms cross at a single point which is independent of size for the same reasons explained above. The cluster algorithm averages over the three Gaussian distributions thus destroying the hysteresis. Since at the coexistence fields the minimum of the distribution is at a fixed point, independent of lattice size, the averaged densities at these fields will also be independent of system size.

[1] L. D. Landau and E. M. Lifshitz, *Statistical Mechanics* (Pergamon, Oxford, England, 1958).
[2] N. Metropolis, A. W. Rosenbluth, M. N. Rosenbluth, and A. H. Teller, J. Chem. Phys. **21**, 1087 (1953).
[3] R. J. Glauber, J. Math. Phys. **4**, 294 (1963).
[4] U. Wolff, Phys. Rev. Lett. **62**, 361 (1989).
[5] R. H. Swendsen and J. S. Wang, Phys. Rev. Lett. **58**, 86 (1987).
[6] K. Kawasaki, in *Phase Transitions and Critical Phenomena*, edited by C. Domb and M. S. Green (Academic, London, 1972), Vol. 2, p. 443.
[7] C. S. Shida and V. B. Henriques, J. Chem. Phys. **115**, 8655 (2001).
[8] C. S. Shida, V. B. Henriques, and M. J. de Oliveira, Phys. Rev. E **68**, 066125 (2003).
[9] M. Girardi, V. B. Henriques, and W. Figueiredo, Chem. Phys. **316**, 117 (2005).

[10] B. A. Berg and T. Neuhaus, Phys. Lett. B **267**, 249 (1991); Phys. Rev. Lett. **68**, 9 (1992).
[11] E. Marinari and G. Parisi, Europhys. Lett. **19**, 451 (1992).
[12] M. B. Bouabci and C. E. I. Carneiro, Phys. Rev. B **54**, 359 (1996).
[13] M. Blume, V. J. Emery, and R. B. Griffiths, Phys. Rev. A **4**, 1071 (1971).
[14] W. Hoston and A. N. Berker, Phys. Rev. Lett. **67**, 1027 (1991).
[15] B. Widom, J. Chem. Phys. **39**, 2808 (1963).
[16] M. J. de Oliveira, Phys. Lett. A **91**, 234 (1982).
[17] M. Creutz, Phys. Rev. Lett. **50**, 1411 (1983).
[18] W. M. Lang and D. Stauffer, J. Phys. A **20**, 5413 (1987).
[19] Loop is an expression borrowed from the mean field theory to characterize a region of thermodynamic instability. In our case, the origin of loops is the finite size effects of the system.
[20] C. E. Fiore, Master dissertation, University of São Paulo, 2003.
[21] M. S. S. Challa, D. P. Landau, and K. Binder, Phys. Rev. B **34**, 1841 (1986).
[22] R. C. Desai, D. W. Heermann, and K. Binder, J. Stat. Phys. **53**, 795 (1988).
[23] T. L. Hill, *Statistical Mechanics: Principles and Selected Applications* (Dover, New York, 1987).
[24] D. P. Landau, in *Finite Size Scaling and Numerical Simulation of Statistical Systems*, edited by V. Privman (World Scientific, Singapore, 1990), p. 223.
[25] K. Binder and D. W. Heermann, *Monte Carlo Simulation in Statistical Physics: An introduction* (Springer, Heidelberg, 2002).